

Supporting Information to

Extensive Molecular Dynamics Simulations Showing That Canonical G8 and Protonated A38H⁺ Forms Are Most Consistent with Crystal Structures of Hairpin Ribozyme

Vojtěch Mlýnský, Pavel Banáš, Daniel Hollas, Kamila Réblová, Nils G. Walter, Jiří Šponer and Michal Otyepka

1) Parameters of non-standard residues

Four non-standard residues (Fig. S1) were used in presented simulations: N1-deprotonated guanine (RGM), N1-protonated adenine (RAP), guanine-N1,O6-enol tautomer (RGT) and 2'-methoxyadenine (RMA).

The N9-methyl-N1-deprotonated guanine, N9-methyl-N1-protonated adenine and N9-methyl guanine-N1,O6-enol tautomer were fully geometrically optimized at HF/6-31G(d) level of theory using the Gaussian03 program¹ and subsequently used for parameterization of negatively charged deprotonated guanine, protonated adenine and guanine enol tautomer, respectively. The partial atomic charges of all non-standard bases were assigned by the restrained electrostatic potential (RESP) fit procedure at HF/6-31G(d) level of theory according to the scheme of Cornell *et al.*^{2,3} The non-standard bases were merged with the corresponding standard parm99 nucleoside residues to obtain topologies for non-standard nucleosides. The N9-methyl atom was replaced by the C1' carbon atom and the residual fractional charge was added to the C1' carbon.

The 2',5'-bismethoxyadenosine-3'-methylmonophosphate model was used to obtain partial atomic charges of 2'-methoxyadenine. The conformation of the methyl-3'-deoxyadenosine-2'-methylmonophosphate modeling 2'-methoxyadenine was derived from the crystal structure (PDB ID 2OUE).⁴ The methyl-3'-deoxyadenosine-2'-methylmonophosphate was geometrically optimized at HF/6-31G(d) level of theory using the Gaussian03 program. All sugar-phosphate backbone torsions were constrained during the optimization to retain the conformation of model close to the crystal structure geometry. Subsequently, the partial atomic charges were determined using RESP procedure at HF/6-31G(d) level of theory. The obtained partial RESP charges of C2' and C3' atoms and atoms of their substituents were pasted to parm99 adenine residue and the residual fractional charges were added to C2', C3' carbons.

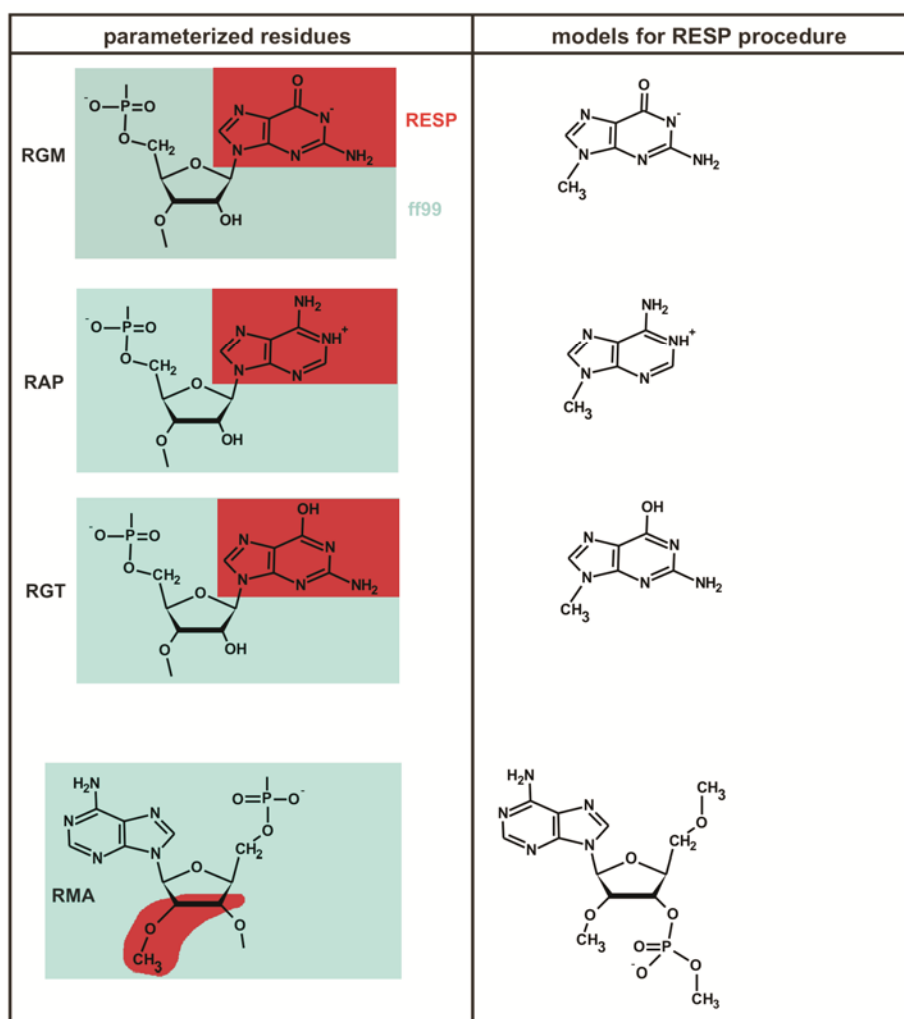


Figure S1: Left panel shows structures of non-standard residues and right panel models, used for calculation of RESP charges. Whereas cyan insets on the left panel illustrate atoms with default parm99 charges, red insets show atoms, which partial charges were derived from RESP procedure.

a) AMBER prep file for 2'-methoxy form of adenine (MRA).

```

0      0      2
This is a remark line
molecule.res
MRA      XYZ      0
CHANGE      OMIT DU      BEG
0.0000
1  DUMM  DU      M      999.000      999.0      -999.0      .00000
2  DUMM  DU      M      999.000      -999.0      999.0      .00000
3  DUMM  DU      M      -999.000      999.0      999.0      .00000
4  P      P      M      2.314000      1.777000      -0.478000      1.16620
5  O1P   O2      E      1.933000      3.073000      -1.082000      -0.77600
6  O2P   O2      E      3.157000      0.872000      -1.292000      -0.77600
7  O5'   OS      M      2.994000      2.142000      0.923000      -0.49890
8  C5'   CT      M      2.156000      2.552000      2.020000      0.05580
9  H5'1  H1      E      1.453000      1.754000      2.258000      0.06790
10 H5'2  H1      E      1.605000      3.450000      1.741000      0.06790
11 C4'   CT      M      3.008000      2.848000      3.243000      0.10650
12 H4'   H1      E      2.447000      3.477000      3.934000      0.11740

```

13	O4'	OS	S	3.228000	1.605000	3.977000	-0.35480
14	C1'	CT	B	4.559000	1.151000	3.778000	0.03940
15	H1'	H2	E	5.072000	1.095000	4.737000	0.20070
16	N9	N*	S	4.539000	-0.297000	3.316000	-0.02510
17	C8	CK	B	4.337000	-0.846000	2.077000	0.20060
18	H8	H5	E	4.152000	-0.207000	1.226000	0.15530
19	N7	NB	S	4.453000	-2.141000	2.049000	-0.60730
20	C5	CB	S	4.754000	-2.480000	3.363000	0.05150
21	C6	CA	B	4.998000	-3.708000	3.989000	0.70090
22	N6	N2	B	4.977000	-4.883000	3.346000	-0.90190
23	H61	H	E	5.161000	-5.739000	3.851000	0.41150
24	H62	H	E	4.777000	-4.914000	2.356000	0.41150
25	N1	NC	S	5.265000	-3.689000	5.302000	-0.76150
26	C2	CQ	B	5.285000	-2.520000	5.935000	0.58750
27	H2	H5	E	5.498000	-2.482000	6.993000	0.04730
28	N3	NC	S	5.073000	-1.309000	5.456000	-0.69970
29	C4	CB	E	4.806000	-1.356000	4.133000	0.30530
30	C3'	CT	M	4.416000	3.378000	2.961000	0.02368
31	H3'	H1	E	4.412000	3.941000	2.028000	0.14322
32	C2'	CT	B	5.230000	2.096000	2.779000	0.07929
33	H2	H1	E	5.668000	2.081000	1.781000	0.12625
34	O2'	OS	S	6.273000	2.050000	3.757000	-0.33043
35	CM'	CT	3	6.759000	1.235000	3.611000	0.01050
36	H2'1	H1	E	6.733287	0.539551	4.456873	0.06003
37	H2'2	H1	E	7.790229	1.577426	3.701673	0.06003
38	H2'3	H1	E	6.835622	0.719500	2.636731	0.06003
39	O3'	OS	M	5.030000	4.129000	3.998000	-0.52460

LOOP

C1' C2'
C4 N9
C4 C5

IMPROPER

C4 C8 N9 C1'
H8 N9 C8 N7
C6 C4 C5 N7
C5 N6 C6 N1
C6 H61 N6 H62
H2 N1 C2 N3
C5 N9 C4 N3

DONE

STOP

b) AMBER prep file for deprotonated guanine residue (RGM)

0 0 2

This is a remark line

molecule.res

RGM XYZ 0

CHANGE OMIT DU BEG

0.0000

1	DUMM	DU	M	0	-1	-2	0.00	0.00	0.00	0.0000
2	DUMM	DU	M	1	0	-1	1.00	0.00	0.00	0.0000
3	DUMM	DU	M	2	1	0	1.00	90.00	0.00	0.0000
4	P	P	M	3	2	1	1.60	119.04	200.00	1.1662
5	O1P	O2	E	4	3	2	1.48	109.61	150.00	-0.7760
6	O2P	O2	E	4	3	2	1.48	109.58	20.00	-0.7760
7	O5'	OS	M	4	3	2	1.60	101.43	-98.89	-0.4989
8	C5'	CT	M	7	4	3	1.44	119.00	-39.22	0.0558
9	H5'1	H1	E	8	7	4	1.09	109.50	60.00	0.0679
10	H5'2	H1	E	8	7	4	1.09	109.50	-60.00	0.0679
11	C4'	CT	M	8	7	4	1.52	110.00	180.00	0.1065
12	H4'	H1	E	11	8	7	1.09	109.50	-200.00	0.1174
13	O4'	OS	S	11	8	7	1.46	108.86	-86.31	-0.3548
14	C1'	CT	B	13	11	8	1.42	110.04	105.60	-0.0227

15	H1'	H2	E	14	13	11	1.09	109.50	-240.00	0.2006
16	N9	N*	S	14	13	11	1.49	108.06	-127.70	0.0005
17	C8	CK	B	16	14	13	1.38	129.20	81.59	0.0125
18	H8	H5	E	17	16	14	1.08	120.00	0.00	0.1339
19	N7	NB	S	17	16	14	1.31	114.00	-179.90	-0.5521
20	C5	CB	S	19	17	16	1.39	103.90	0.00	-0.0301
21	C6	C	B	20	19	17	1.42	130.40	180.00	0.7707
22	O6	O	E	21	20	19	1.23	128.80	0.00	-0.7034
23	N1	NC	S	21	20	19	1.40	111.38	180.00	-0.8744
24	C2	CA	B	23	21	20	1.38	125.24	-0.10	0.9143
25	N2	N2	B	24	23	21	1.34	116.02	180.00	-0.9610
26	H21	H	E	25	24	23	1.01	127.00	-0.82	0.3573
27	H22	H	E	25	24	23	1.01	116.53	-179.44	0.3573
28	N3	NC	S	24	23	21	1.33	123.30	0.00	-0.8208
29	C4	CB	E	28	24	23	1.36	112.20	0.00	0.3334
30	C3'	CT	M	11	8	7	1.53	115.78	-329.11	0.2022
31	H3'	H1	E	30	11	8	1.09	109.50	30.00	0.0615
32	C2'	CT	B	30	11	8	1.53	102.80	-86.30	0.0670
33	H2'1	H1	E	32	30	11	1.09	109.50	120.00	0.0972
34	O2'	OH	S	32	30	11	1.43	109.50	240.00	-0.6139
35	HO'2	HO	E	34	32	30	0.96	107.00	180.00	0.4186
36	O3'	OS	M	30	11	8	1.42	116.52	-203.47	-0.5246

IMPROPER

C8 C4 N9 C1'
 C5 N1 C6 O6
 C2 H21 N2 H22
 N7 N9 C8 H8
 N1 N3 C2 N2

LOOP CLOSING EXPLICIT

C1' C2'
 C4 C5
 C4 N9

DONE
 STOP

c) AMBER prep file for O6H G8 tautomer (RGT)

0 0 2

R-GUANINE - with 5' - phosphate group and 3' - O(minus) group

RGT	INT	1									
CORRECT	OMIT	DU	BEG								
0.0											
1	DUMM	DU	M	0	-1	-2	0.00	0.00	0.00	0.0000	
2	DUMM	DU	M	1	0	-1	1.00	0.00	0.00	0.0000	
3	DUMM	DU	M	2	1	0	1.00	90.00	0.00	0.0000	
4	P	P	M	3	2	1	1.60	119.04	200.00	1.1662	
5	O1P	O2	E	4	3	2	1.48	109.61	150.00	-0.7760	
6	O2P	O2	E	4	3	2	1.48	109.58	20.00	-0.7760	
7	O5'	OS	M	4	3	2	1.60	101.43	-98.89	-0.4989	
8	C5'	CT	M	7	4	3	1.44	119.00	-39.22	0.0558	
9	H5'1	H1	E	8	7	4	1.09	109.50	60.00	0.0679	
10	H5'2	H1	E	8	7	4	1.09	109.50	-60.00	0.0679	
11	C4'	CT	M	8	7	4	1.52	110.00	180.00	0.1065	
12	H4'	H1	E	11	8	7	1.09	109.50	-200.00	0.1174	
13	O4'	OS	S	11	8	7	1.46	108.86	-86.31	-0.3548	
14	C1'	CT	B	13	11	8	1.42	110.04	105.60	0.0289	
15	H1'	H2	E	14	13	11	1.09	109.50	-240.00	0.2006	
16	N9	N*	S	14	13	11	1.49	108.06	-127.70	0.0020	
17	C8	CK	B	16	14	13	1.38	127.98	81.59	0.0554	
18	H8	H5	E	17	16	14	1.08	120.47	0.00	0.1786	
19	N7	NB	S	17	16	14	1.28	114.44	-179.90	-0.5110	
20	C5	CB	S	19	17	16	1.39	103.90	0.00	0.0332	
21	C6	C	B	20	19	17	1.39	134.97	180.00	0.6339	
22	O6	OH	S	21	20	19	1.32	121.30	0.00	-0.5751	

23	H1	HO	E	22	21	20	0.95	108.10	180.00	0.4448
24	N1	NC	S	21	20	19	1.31	120.51	180.00	-0.7821
25	C2	CA	B	24	21	20	1.34	118.67	-0.10	0.8950
26	N2	N2	B	25	24	21	1.36	115.62	180.00	-0.9120
27	H21	H	E	26	25	24	1.00	116.70	-0.82	0.3897
28	H22	H	E	26	25	24	1.00	116.70	-179.44	0.3897
29	N3	NC	S	25	23	21	1.32	127.02	0.00	-0.7190
30	C4	CB	E	29	25	24	1.33	112.30	0.00	0.3634
31	C3'	CT	M	11	8	7	1.53	115.78	-329.11	0.2022
32	H3'	H1	E	31	11	8	1.09	109.50	30.00	0.0615
33	C2'	CT	B	31	11	8	1.53	102.80	-86.30	0.0670
34	H2'1	H1	E	33	31	11	1.09	109.50	120.00	0.0972
35	O2'	OH	S	33	31	11	1.43	109.50	240.00	-0.6139
36	HO'2	HO	E	35	33	31	0.96	107.00	180.00	0.4186
37	O3'	OS	M	31	11	8	1.42	116.52	-203.47	-0.5246

IMPROPER

C8	C4	N9	C1'
C5	N1	C6	O6
C6	C2	N1	H1
C2	H21	N2	H22
N7	N9	C8	H8
N1	N3	C2	N2

LOOP CLOSING EXPLICIT

C1'	C2'
C4	C5
C4	N9

DONE

STOP

d) AMBER prep file for protonated adenine (RAP)

0 0 2

This is a remark line

molecule.res

RAP XYZ 0

CHANGE OMIT DU BEG

0.0000

1	DUMM	DU	M	0	-1	-2	0.00	0.00	0.00	0.0000
2	DUMM	DU	M	1	0	-1	1.00	0.00	0.00	0.0000
3	DUMM	DU	M	2	1	0	1.00	90.00	0.00	0.0000
4	P	P	M	3	2	1	1.60	119.04	200.00	1.1662
5	O1P	O2	E	4	3	2	1.48	109.61	150.00	-0.7760
6	O2P	O2	E	4	3	2	1.48	109.58	20.00	-0.7760
7	O5'	OS	M	4	3	2	1.60	101.43	-98.89	-0.4989
8	C5'	CT	M	7	4	3	1.44	119.00	-39.22	0.0558
9	H5'1	H1	E	8	7	4	1.09	109.50	60.00	0.0679
10	H5'2	H1	E	8	7	4	1.09	109.50	-60.00	0.0679
11	C4'	CT	M	8	7	4	1.52	110.00	180.00	0.1065
12	H4'	H1	E	11	8	7	1.09	109.50	-200.00	0.1174
13	O4'	OS	S	11	8	7	1.46	108.86	-86.31	-0.3548
14	C1'	CT	B	13	11	8	1.42	110.04	105.60	0.1297
15	H1'	H2	E	14	13	11	1.09	109.50	-240.00	0.2007
16	N9	N*	S	14	13	11	1.52	109.59	-127.70	-0.0532
17	C8	CK	B	16	14	13	1.37	131.20	81.59	0.1412
18	H8	H5	E	17	16	14	1.08	120.00	0.00	0.2008
19	N7	NB	S	17	16	14	1.30	113.93	177.00	-0.5330
20	C5	CB	S	19	17	16	1.39	104.00	0.00	0.2613
21	C6	CA	B	20	19	17	1.40	132.42	180.00	0.2748
22	N6	N2	B	21	20	19	1.34	123.50	0.00	-0.7251
23	H61	H	E	22	21	20	1.01	120.00	180.00	0.4282
24	H62	H	E	22	21	20	1.01	120.00	0.00	0.4282
25	N1	NA	B	21	20	19	1.34	117.43	180.00	-0.2604
26	H1	H	E	25	21	20	1.00	119.46	180.00	0.3566
27	C2	CQ	B	25	21	20	1.33	118.80	0.00	0.1964
28	H2	H5	E	27	25	21	1.08	120.00	180.00	0.1889

29	N3	NC	S	27	25	21	1.32	129.17	0.00	-0.4431
30	C4	CB	E	29	27	25	1.35	110.80	0.00	0.3240
31	C3'	CT	M	11	8	7	1.53	115.78	-329.11	0.2022
32	H3'	H1	E	31	11	8	1.09	109.50	30.00	0.0615
33	C2'	CT	B	31	11	8	1.53	102.80	-86.30	0.0670
34	H2'1	H1	E	33	31	11	1.09	109.50	120.00	0.0972
35	O2'	OH	S	33	31	11	1.43	109.50	240.00	-0.6139
36	HO'2	HO	E	35	33	31	0.96	107.00	180.00	0.4186
37	O3'	OS	M	31	11	8	1.42	116.52	-203.47	-0.5246

IMPROPER

```
C8 C4 N9 C1'
C6 H61 N6 H62
N7 N9 C8 H8
N1 N3 C2 H2
C5 N1 C6 N6
C6 C2 N1 H1
```

LOOP CLOSING EXPLICIT

```
C1' C2'
C4 C5
C4 N9
```

DONE

STOP

e) AMBER parm file non-standard parameters

force field modification for RMA, RGM, RGT, RAP, IN1, IN2, and L25 residues

MASS

```
OX 16.00 0.465 based on OS ether and ester oxygen
HX 1.008 0.135 based on HO hydroxyl group
```

BOND

```
CT-OX 320.0 1.410 based on CT-OS JCC,7, (1986),230; NUCLEIC ACIDS
HX-OH 553.0 0.960 based on HO-OH JCC,7, (1986),230; SUGARS,SER,TYR
CQ-NA 502.0 1.324 based on CQ-NC JCC,7, (1986),230; ADE
```

ANGLE

```
H1-CT-OX 50.0 109.50 based on H1-CT-OS changed based on NMA nmodes
CT-CT-OX 50.0 109.50 based on CT-CT-OS
CB-CA-NA 70.0 117.30 based on CB-CA-NC
NC-CQ-NA 70.0 129.10 based on NC-CQ-NC
H5-CQ-NA 50.0 115.45 based on H5-CQ-NC
CA-NA-CQ 70.0 118.60 based on CA-NC-CQ
CQ-NA-H 50.0 118.00 based on CA-NA-H changed based on NMA nmodes
```

DIHEDRAL

```
OX-CT-CT-OS 1 0.144 0.0 -3. based on OS-CT-CT-OS parm98, TC,PC,PAK
OX-CT-CT-OS 1 1.175 0.0 2. based on OS-CT-CT-OS Piotr et al.
H1-CT-CT-OX 1 0.25 0.0 1. based on H1-CT-CT-OS Junmei et al, 1999
OX-CT-CT-OH 1 0.144 0.0 -3. based on OS-CT-CT-OH parm98, TC,PC,PAK
OX-CT-CT-OH 1 1.175 0.0 2. based on OS-CT-CT-OH parm98, TC,PC,PAK
X -NA-CQ- X 4 9.60 80.0 2.
```

NONBON

```
OX 1.6837 0.1700 based on OS OPLS ether
HX 0.6000 0.0157 based on HS W. Cornell CH3SH --> CH3OH FEP
```

2) Behavior of S-turn backbone

The torsion angle analysis of bases making the S-turn region (residues G36, U37, A38, C39, A40) was carried out for the detailed characterization of the S-turn behavior in four chosen simulations (Table S1). Generally, the simulations with canonical A38 showed significantly more dynamical behavior compared to systems with protonated A38H⁺.

We observed α/γ flips of phosphates of all S-turn nucleobases except C39. Most of these α/γ flips appeared for U37 and A38/A38H⁺. The most frequent flips were observed in

WT1/G8/A38 simulation, while only short-term flips occurred for U37, A38 bases in OMe/G8/A38 simulation. In contrast, three longer-time flips occurred for U37 nucleobase in OMe/G8/A38H⁺ simulation.

The dihedral β was stable and unchanged at $\sim 180^\circ$ in nearly all described simulations (Table S1), except of U37 nucleobase in WT1/G8/A38 and WT1/G8/A38H⁺ systems, where it oscillated between two substates with dihedral β values $\sim 180^\circ$ and $\sim 80^\circ$. Notably, we observed also a 5 ns-long flip of dihedral β (from 180° to 80° and back) for G36 in OMe/G8/A38 simulation.

The δ dihedral was rather unchanged in both simulations with protonated A38H⁺, however, residues adjacent to A38 within S-turn changed often their typical δ torsions 150° towards 80° in simulations with canonical A38 (Table S1). Similarly, the sugar puckering of S-turn nucleobases was preferentially C2'-endo in agreement with the initial crystal structures in case of systems with protonated A38H⁺, while sugar pucker of U37 changed from C2'-endo to C3'-endo at ~ 4 ns in WT1/G8/A38, ~ 20 ns in OMe/G8/A38 simulation.

The ϵ and ζ dihedrals were stable (fluctuating around $\sim 90^\circ$) for A38/A38H⁺, and A40 nucleobases. On contrary, ϵ and ζ of G36, U37 and C39 showed a coupled dynamic behavior with a lot of flips, and were fluctuated typically around values $\sim 90^\circ$, $\sim 180^\circ$ and $\sim 270^\circ$. The most ϵ/ζ flips were observed in both simulation with canonical A38 (WT1/G8/A38 and OMe/G8/A38), while the G36 in WT1/G8/A38H⁺ simulations was the only nucleobase carrying ϵ/ζ flips.

3) Supplementary tables

Table S1: Summary of changes in dihedral angles of bases (G36, U37, A38, C39 and A40) within the S-turn region. Nucleobases that underwent dynamical flips in torsion angles are listed (see text for detailed description).

Simulation	dihedrals			
	$\alpha - \gamma$	β	δ	$\epsilon + \zeta$
OMe/G8/A38	G36, U37, A38, A40	G36	G36, U37, C39	G36, U37, C39
OMe/G8/A38H ⁺	U37, A38H ⁺			
WT1/G8/A38	G36, U37, A38, A40	U37	U37, C39	G36, U37, C39
WT1/G8/A38H ⁺	U37, A38H ⁺	U37		G36

Table S2: Table summarizes population of active-site conformation with favorable in-line attack angle (IAA, >130°) and population of A-1(2'-OH) or A-1(2'-OMe) group in the X-ray-like conformation of A-1(2'-OMe) (see Fig. 3A). Populations are averaged over the whole simulation times.

Simulation	IAA (%)	2'-OMe- like (%)	Simulation	IAA (%)	2'-OMe- like (%)
WT/G8 ⁻ /A38	2	0	WT2/G8/A38	3	9
WT/G8 ⁻ /A38H ⁺	3	0	WT1/G8/A38H ⁺	39	2
WT/G8t/A38	7	9	WT2/G8/A38H ⁺	65	0
WT/G8t/A38H ⁺	6	1	WT/G8/A38/ES	2	3
OMe/G8/A38	7	100	WT/G8/A38H ⁺ /ES	4	0
OMe/G8/A38H ⁺	10	100	WT/G8/A38/bsc0	68	81
WT1/G8/A38	49	30	WT/G8/A38H ⁺ /bsc0	35	0

Table S3: Populations of the effective reaction conformation (ERC, Fig. S4) averaged over the whole simulation times.

Simulation	ERC (%)	Simulation	ERC (%)
WT1/G8/A38	1	WT/G8/A38/ES	0
WT2/G8/A38	1	WT/G8/A38H ⁺ /ES	4
WT1/G8/A38H ⁺	18	WT/G8/A38/bsc0	0
WT2/G8/A38H ⁺	65	WT/G8/A38H ⁺ /bsc0	35

Table S4: Times when the 'ladder-like' transition in H4 A-RNA duplex appeared.

Simulation	Time (ns)	Simulation	Time (ns)
WT/G8 ⁻ /A38	-	WT1/2/G8/A38	-
WT/G8 ⁻ /A38H ⁺	-	WT1/2/G8/A38H ⁺	-
WT/G8t/A38	-	WT/G8/A38/ES	-
WT/G8t/A38H ⁺	7	WT/G8/A38H ⁺ /ES	-
OMe/G8/A38	10	WT/G8/A38/bsc0	29
OMe/G8/A38H ⁺	27	WT/G8/A38H ⁺ /bsc0	-

4) Supplementary figures

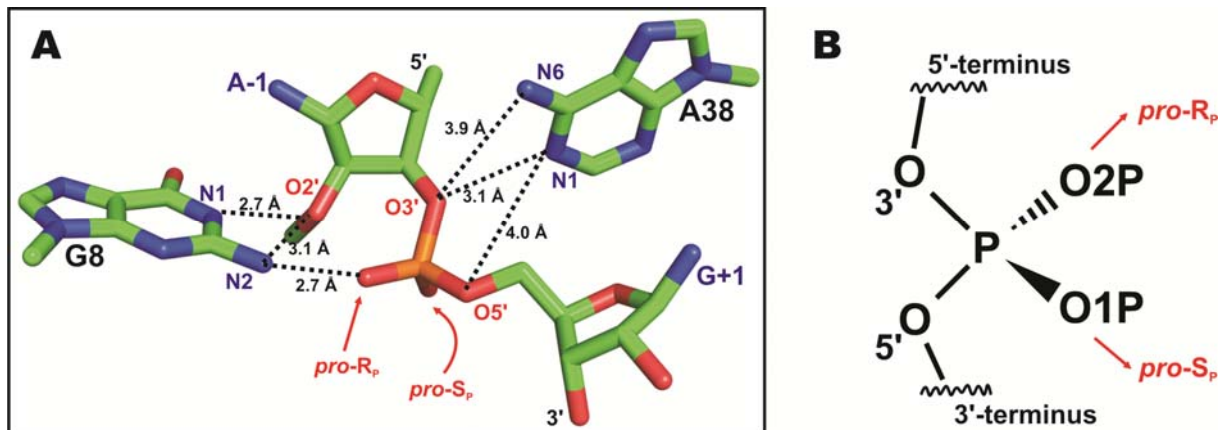


Figure S2: (A) The active site X-ray geometry (PDB ID 2OUE) was used as a starting geometry for MD simulations. Key residues and atoms participating in H-bonds discussed in the text are labeled and lengths of discussed distances are measured. (B) Definition of *pro-R_P*/*pro-S_P* oxygens of the scissile phosphate according to IUPAC terminology.

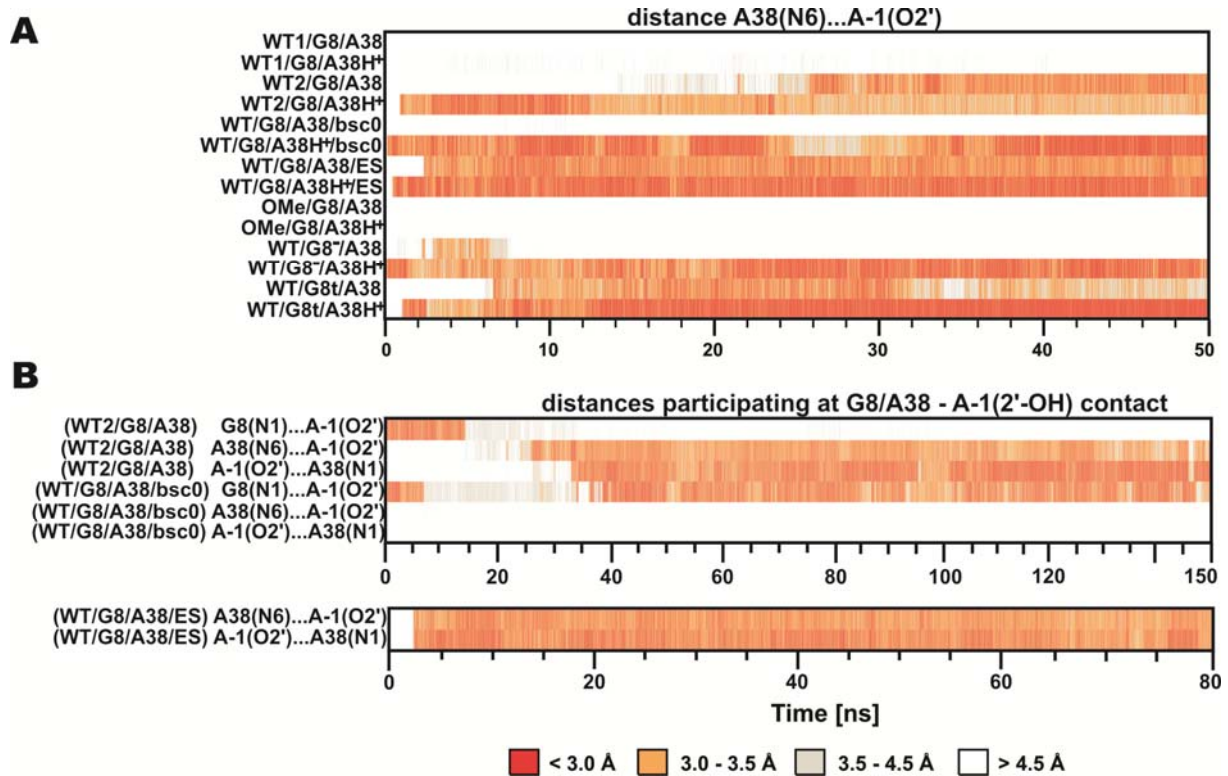


Figure S3: Interatomic distances within the active site. (A) Time evolution of A38(N6)...A-1(O2') distance in all performed MD simulation. (B) Evolution of specific contacts between A38/G8 and A-1(2'-OH) are shown for the entire simulation times of WT2/G8/A38, WT/G8/A38/bsc0 and WT/G8/A38/ES.

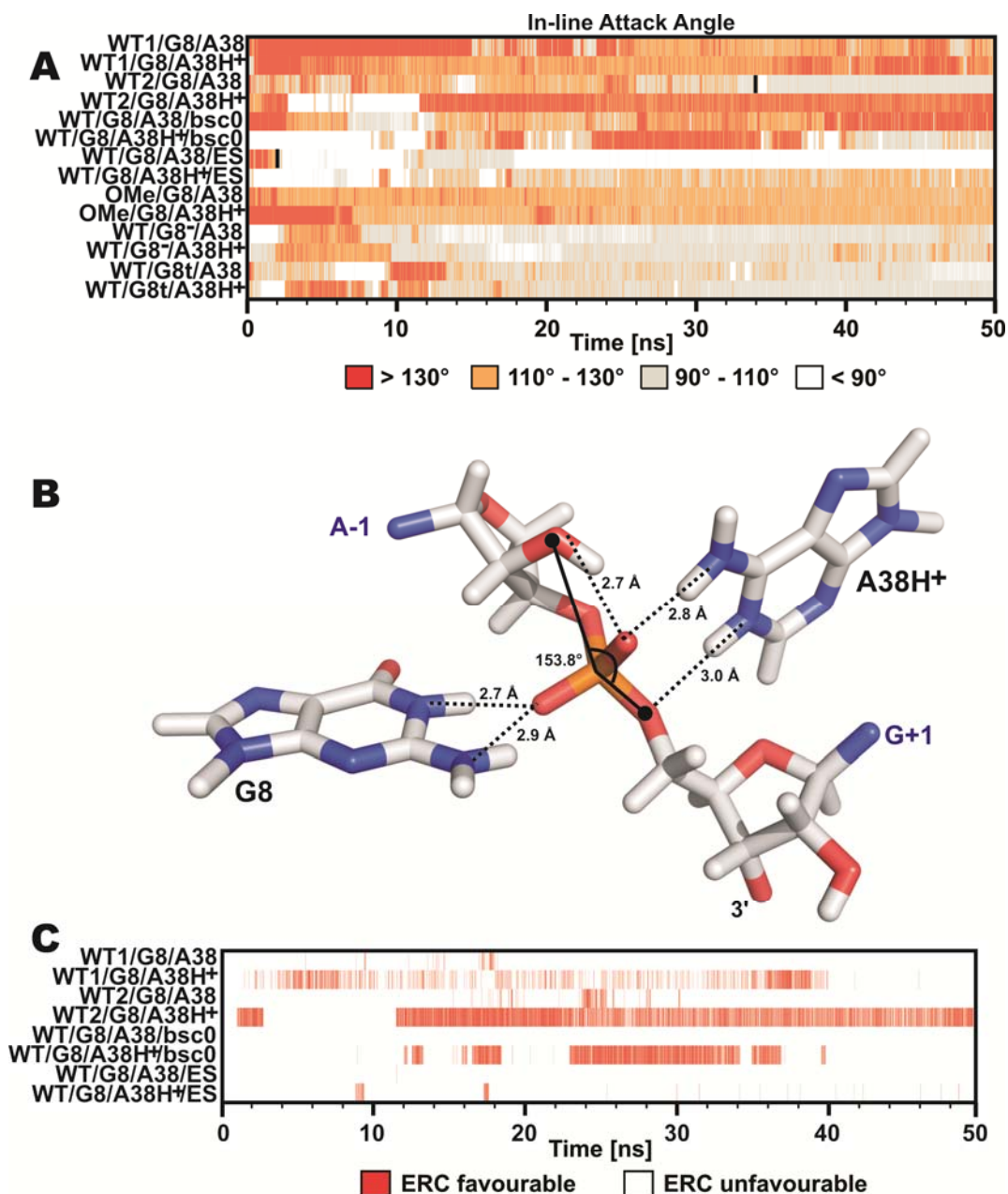


Figure S4: (A) Evolution of the in-line attack angle (IAA, A-1(2'-O)-G+1(P)-G+1(5'-O)). IAA is color-coded as indicated in legend. The IAA higher than 130° is considered as a favorable IAA for the nucleophilic attack of A-1(2'-OH) to the scissile phosphate. The two black dashes inside the plot for WT2/G8/A38 and WT/G8/A38/ES simulations indicate times when A-1(2'-OH)...A38(N1) H-bond was formed. (B) The geometry fulfilling a favorable IAA (>130°) and having contacts between the scissile phosphate and both G8 and A38 (G8(N1)...G+1(pro-R_P/pro-S_P) < 4.0Å, A38(N1)...G+1(O5') < 4.0Å) seems to be the effective reactive conformation (ERC). The snapshot was taken from WT/G8/A38H⁺/bsc0 simulation. (C) Evolution of ERC, the ERC is indicated by red dashes.

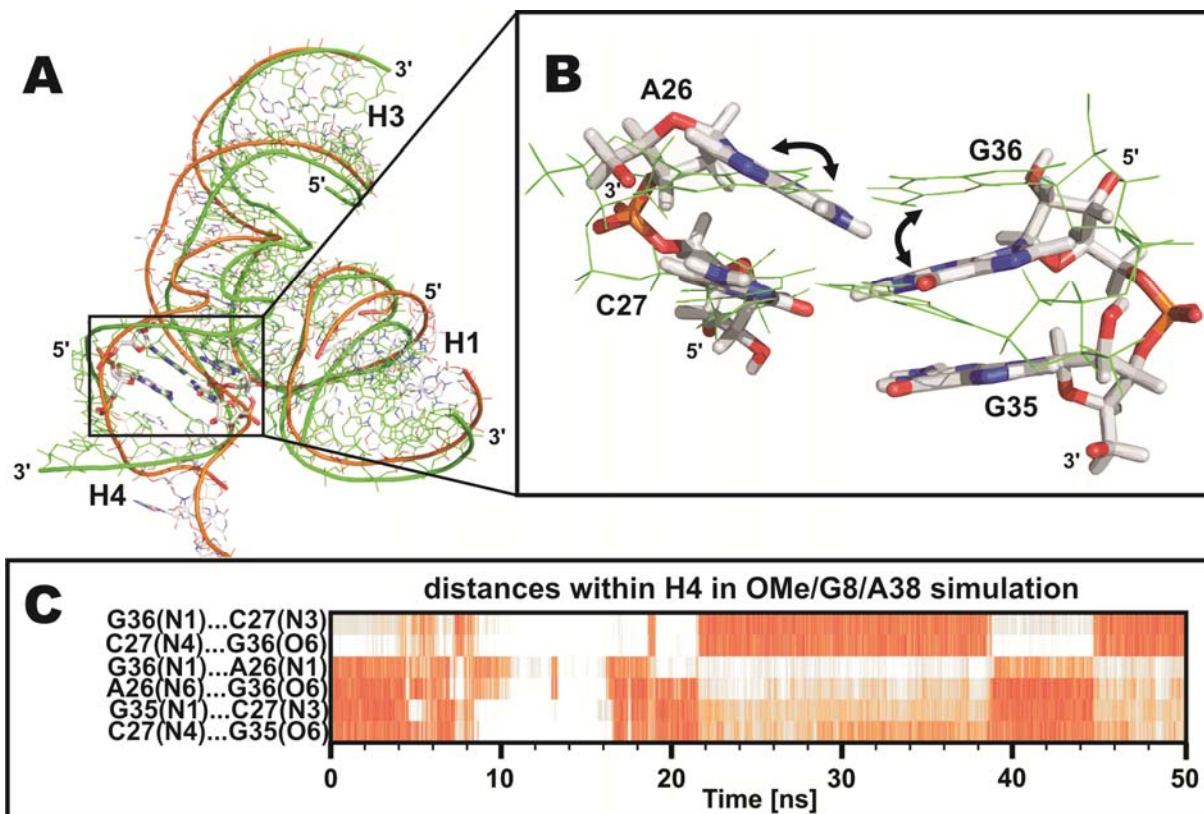


Figure S5: (A) Ribbon diagrams show the hairpin ribozyme with labeled helices H1-H4. (B) The last ns average structure taken from OMe/G8/A38 MD simulations (in sticks) is superimposed with the X-ray geometry (green lines). The G36 nucleobase of H4 interrupts base pair with A26 (black arrows) and creates a new *cis* Watson-Crick base pair with C27, thus displacing G35 out of pairings. (C) The *cis* WC-base pair formation between G36-C27 competes with interactions among G35-C27, G36-A26 nucleobases.

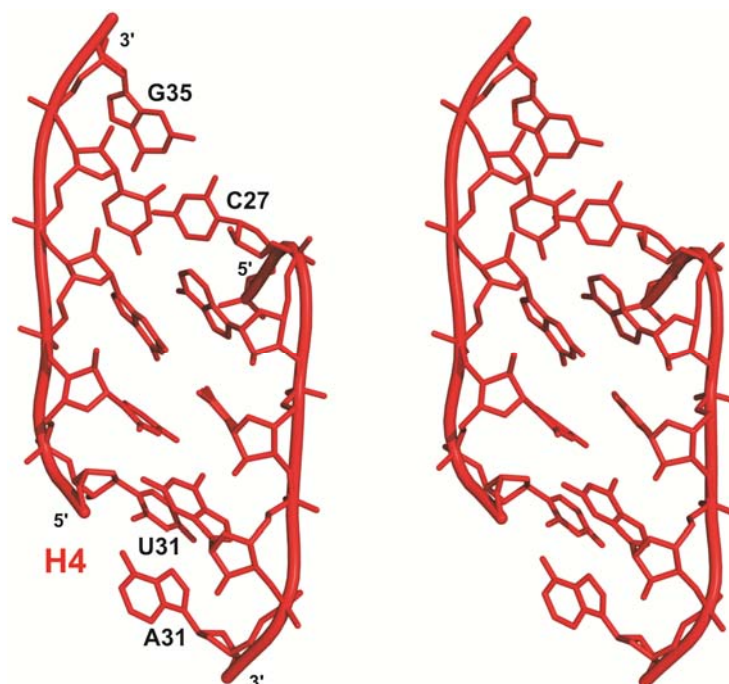


Figure S6: Stereo view of the 'ladder-like' structure of H4 A-RNA duplex taken from OMe/G8/A38H⁺ simulation.

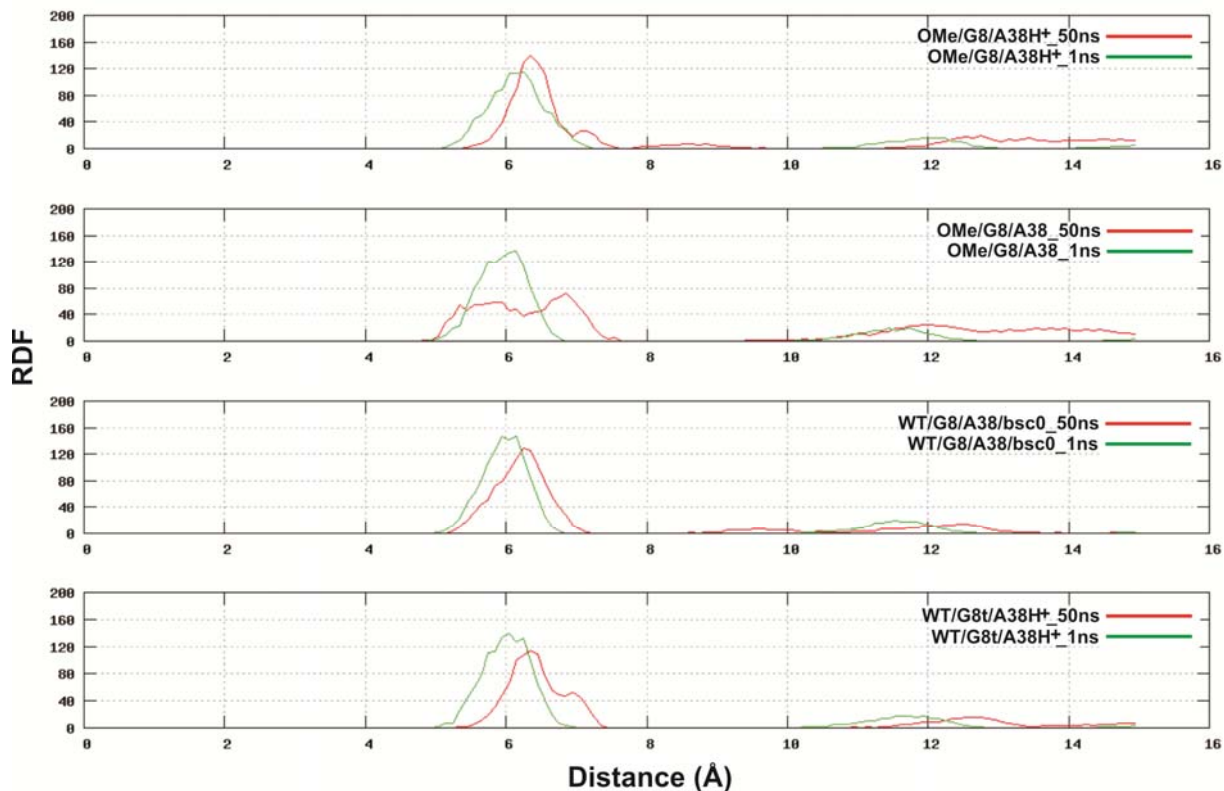


Figure S7: Peaks in P-P radial distribution function (RDF) of 5 basepairs (C27-G35, A28-U34, C29-G33, G30-C32, A31-U31) of H4 shift towards higher values in the 'ladder-like' structures in OMe/G8/A38H⁺, OMe/G8/A38, WT/G8/A38/bsc0 and WT/G8t/A38H⁺ MD simulations. The green line corresponds to the A-RNA conformation and the red one to the 'ladder-like' structure.

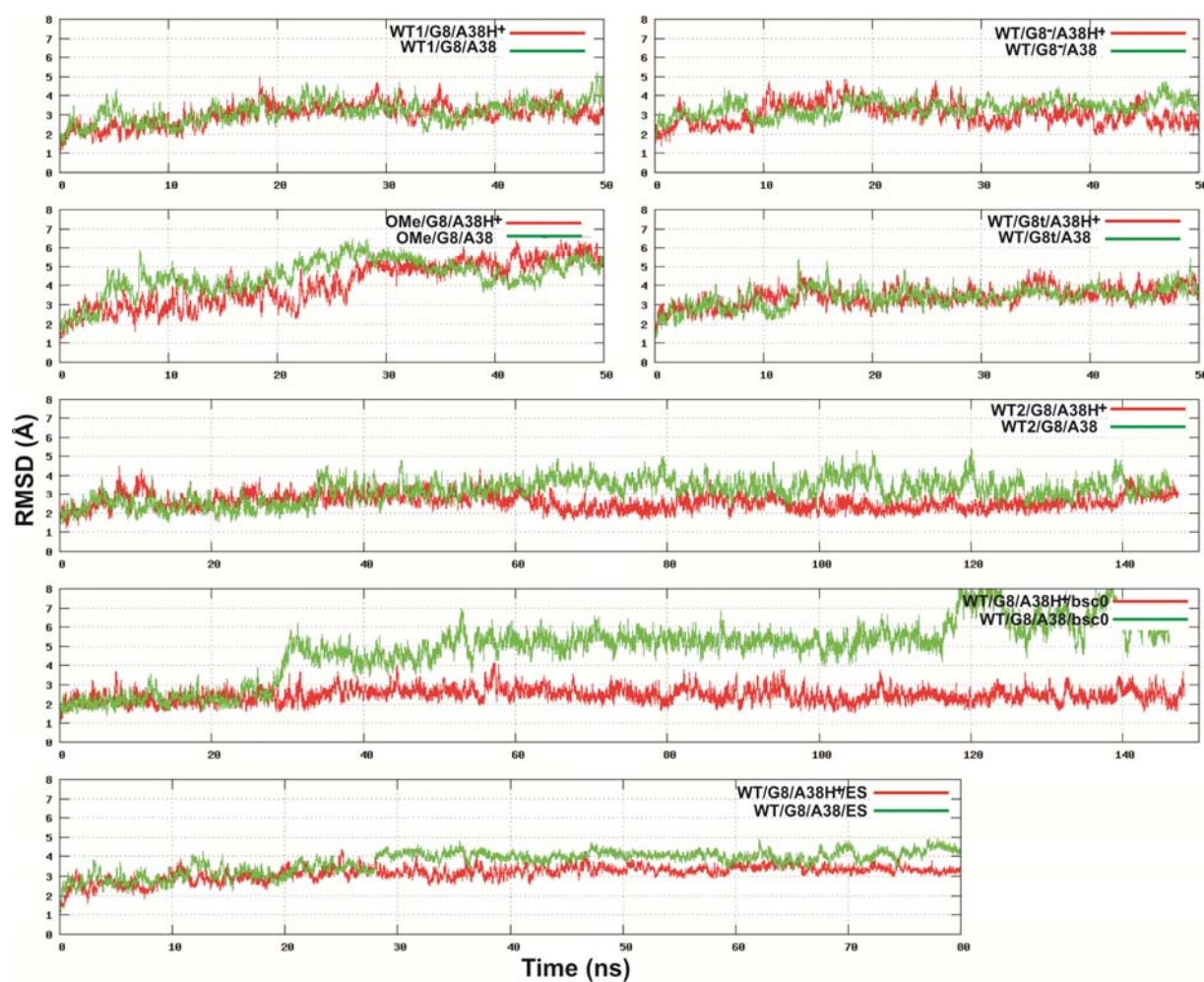


Figure S8: Root mean square deviation (RMSD) of all heavy atoms from the X-ray structure as a function of time for present MD simulations. The green line represents system with canonical A38 and the red line system with protonated A38H⁺ form.

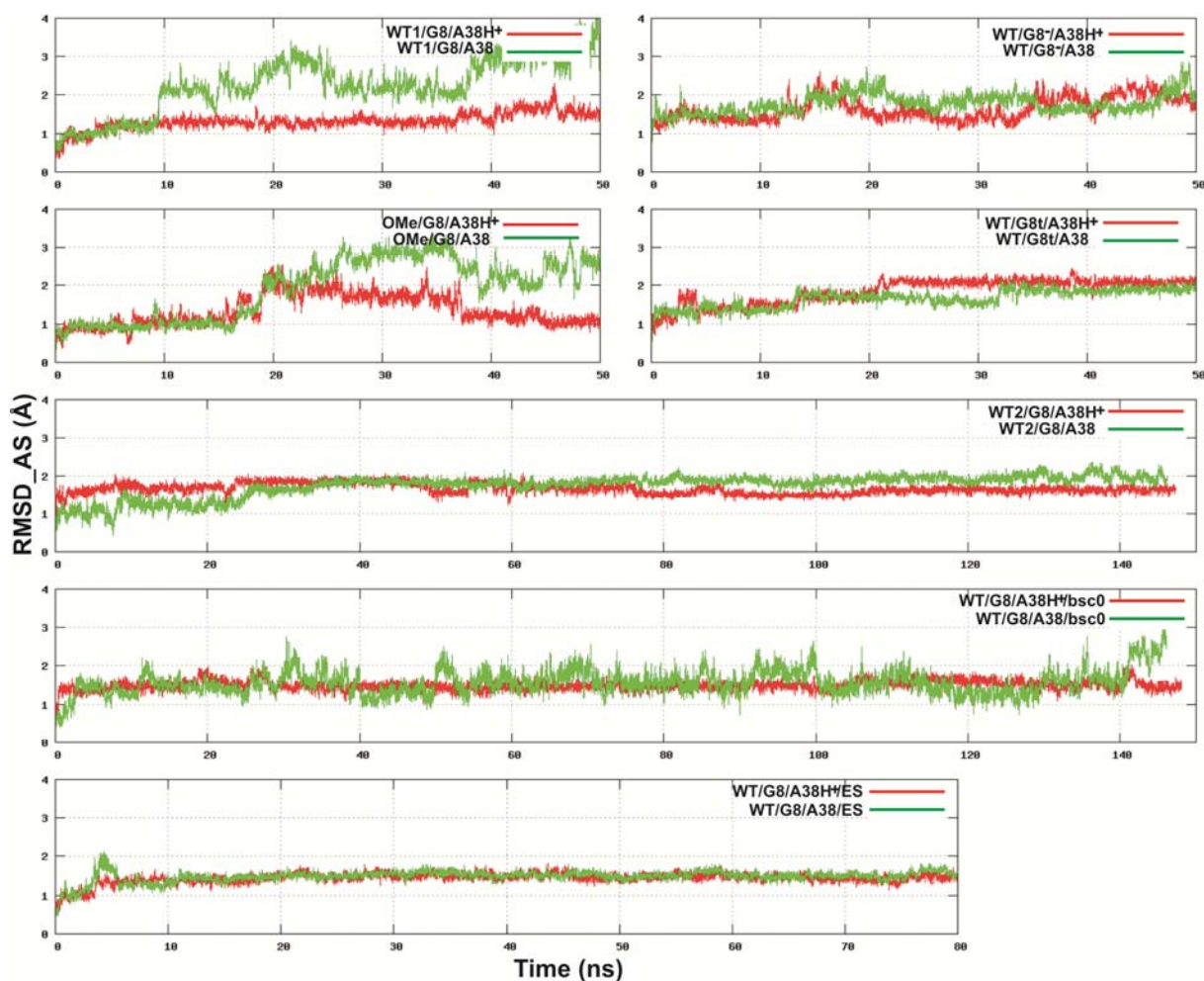


Figure S9. Root mean square deviation (RMSD) of active site (including A-1, G+1, G8 and A38 nucleobases) heavy atoms from the X-ray structure as a function of time for present MD simulations. The green line represents system with canonical A38 and the red line system with protonated A38H⁺ form. Higher RMSD values between 18 and 38 ns in OMe/G8/A38H⁺ simulation (in the system showing best agreement with the X-ray geometry) were caused by temporary expiration of A38H⁺(N1H)...G+1(O5') H-bond.

5) Constant pH Molecular Dynamics

a) Parameterization

We considered two titratable groups in the constant-pH MD simulations: guanine G8 and adenine A38. The parm99 van der Waals parameters of canonical forms of guanosine and adenosine were used for deprotonated state of guanosine and protonated state of adenosine. The charges of canonical forms of both residues were taken from parm99 force field, while the RESP charges were calculated for deprotonated guanosine and protonated adenosine, as described in section Parameters of non-standard residues (see page S1).

The relative energies between each protonation state of given nucleotide calibrating the constant-pH MD method were calculated using thermodynamic integration. The modified generalized Born (GB) model developed by Onufriev, Bashford and Case (*igb=2* in AMBER10 setting) was used in the thermodynamic integration as well as in constant-pH MD simulations. The salt concentration using a modified GB theory based on Debye-Hückel limiting law for ion screening of interactions was set to 0.33 mol·L⁻¹. The twelve-point

Gaussian quadrature was used in thermodynamic integration for evaluation of the free energy difference between protonation forms of titrating residues. In addition to the relative free energies of both protonation forms obtained by thermodynamic integration, the energy of protonated state was increased by $pK_a RT \ln 10$ correction to account pK_a value in the calibration of constant-pH MD. The relative energy corrections of canonical and deprotonated guanine were $9.2 * RT \ln 10$ and 99.49 kcal/mol, respectively. Corrections for protonated and canonical adenine were $3.6 * RT \ln 10$ and 79.94 kcal/mol. Finally, the reference constant-pH MD simulations of model compounds N9-methylguanine/N1-deprotonated-N9-methylguanine and N1-protonated-N9-methyladenine/N9-methyladenine at pH equal to pK_a values of guanosine (pK_a 9.2) and adenosine (pK_a 3.6) were performed to check the set of parameters. The Monte Carlo step was performed every 100 fs in constant-pH MD simulations. We observed a half to half population of protonation states of given nucleobase in the reference constant-pH simulations within precision of 0.1%, as expected for pH equal to pK_a .

b) Reference generalized Born MD simulation

We performed a reference MD simulation utilizing the generalized Born (GB) model to check the stability of RNA structure in the implicit solvent model. Again, the modified GB model (developed by Onufriev, Bashford and Case ($igb=2$ in AMBER10) with the salt concentration using of 0.33 mol/l) was used as a setting of GB implicit model.

The last snapshot of the WT2/G8/A38H⁺ simulation representing well equilibrated system was used as a starting structure. All ions and water molecules were removed and GB implicit solvation model was turned on. Subsequently, the system was minimized using similar minimization protocol as described in the Methods section of the main text. The periodic boundary condition was turned off, cutoff was increased to 30 Å (as recommended in AMBER10 manual) and the GB model with concentration of salt screening was set as described above. The 1-fs -long integration time integration step was used in thermalization and production phases. Finally, the system was slowly heated to 300 K during 100-ps long thermalization phase.

We observed a disastrous structural degradation of the hairpin ribozyme global structure during the first tens of ps of thermalization phase. The structure of the minimal, junction-less hairpin ribozyme was severely perturbed at the end of 100-ps long thermalization and the unfolding of the structure was observed in the following production phase. Addition of explicit monovalent ions did not influence global structural behavior during the GB simulation.

c) The constant-pH MD simulations

To avoid the structural degradation described in the previous paragraph, we applied the harmonic cartesian restrains to all atoms of the hairpin ribozyme to keep them fluctuating around the starting structure corresponding to equilibrium in explicit solvent condition. Subsequently, the series of constant-pH MD simulation at different pHs were carried out to obtain pK_a constants of the two studied titrating groups. We run 18 simulations with pH ranging from 1 to 31. The simulation protocol was the same as described in the previous paragraph using the modified GB model developed by Onufriev, Bashford and Case ($igb=2$ in AMBER10) with the salt concentration 0.33 mol·L⁻¹. The Monte Carlo step was performed each 5 fs and data were collected for 5 ns after thermalization in each pK_a simulation. Finally, the fit to Henderson-Hasselbach equation was used to estimate pK_a constants (Fig. S10).

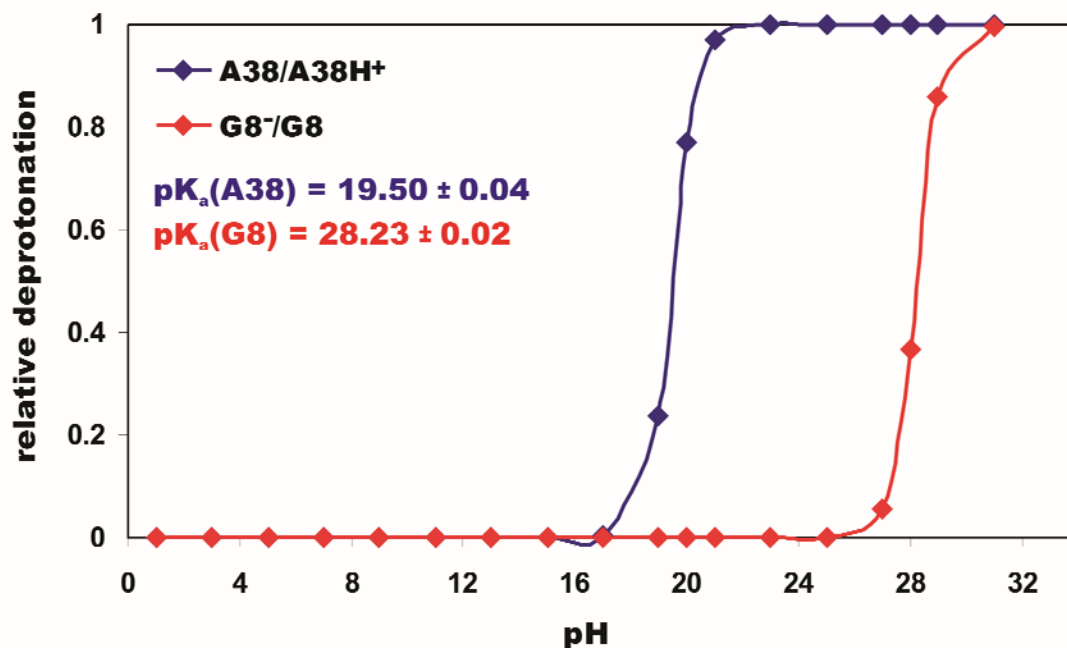


Figure S10. The titration curves obtained from constant pH MD simulations. The blue and red diamonds stand for relative deprotonation of A38H⁺ and guanine G8 at given pH. Obtained pK_a values are indicated in appropriate colors.

References:

- (1) Frisch, M., J.; Frisch, A.; Foresman, J., B. Gaussian 03; Gaussian, Inc.: Pittsburgh, 2003.
- (2) Cornell, W. D.; Cieplak, P.; Bayly, C. I.; Gould, I. R.; Merz, K. M.; Ferguson, D. M.; Spellmeyer, D. C.; Fox, T.; Caldwell, J. W.; Kollman, P. A. *Journal of the American Chemical Society* **1995**, *117*, 5179.
- (3) Cornell, W. D.; Cieplak, P.; Bayly, C. I.; Kollman, P. A. *Journal of the American Chemical Society* **1993**, *115*, 9620.
- (4) Rupert, P. B.; Ferre-D'Amare, A. R. *Nature* **2001**, *410*, 780.